Conformation of Ethyl (+)-(2*S*,3*S*)-3-{1-[*N*-(3-Methylbutyl)amino]leucylcarbonyl}oxirane-2-carboxylate (Loxistatin), a Cysteine Protease Inhibitor: *X*-Ray Crystallographic and ^{1}H Nuclear Magnetic Resonance Studies

Toshimasa Ishida,* Masaaki Sakaguchi, Daisuke Yamamoto, and Masatoshi Inoue
Laboratory of Physical Chemistry, Osaka University of Pharmaceutical Sciences, 2-10-65 Kawai, Matsubara, Osaka 580, Japan
Kunihiro Kitamura, Kazunori Hanada, and Takanao Sadatome
Research Laboratories, Taisho Pharmaceutical Co. Ltd., 1-403 Yoshinocho, Ohmiya, Saitama 330, Japan

In order to establish the conformational characteristics of a cysteine protease inhibitor, the crystal and solution conformations of loxistatin have been determined by *X*-ray crystallographic and ^{1}H n.m.r. spectroscopic analyses. The molecules were arranged in the crystal as a series of infinite parallel β-sheet structures formed *via* intermolecular N-H • • • O hydrogen bonds. The loxistatin molecule has a flattened, curved conformation, which appears to be energetically stable. Similar conformations of loxistatin were also observed in $(CD_3)_2SO$ and $CDCl_3$ solutions. On the basis of the results obtained, the relation between the conformation of loxistatin and its inhibitory activity was discussed and compared with the stereostructure of the papain–substrate analogue complex.

It is increasingly apparent that proteases are important in the initiation, maintenance, and termination of a wide variety of biological processes.[1] The central role of proteolysis in these processes makes the development of specific, selective, non-toxic protease inhibitors an interesting challenge in drug design.

The cysteine proteases have an essential, highly reactive thiol group at their active sites. Papain, cathepsins, and Ca^{2+}-activated neutral protease (CANP) are well known examples. Since these proteases are believed to be important in the degradation of muscle proteins,[2] the development of specific, low molecular weight inhibitors are likely to be of great significance in the treatment of muscular dystrophy.

(+)-(2*S*,3*S*)-3-(1-{*N*-[4-(guanidino)butyl]amino}leucylcarbonyl)oxirane-2-carboxylic acid (**1**) (E-64), isolated from cultures of *Aspergillus japonicus*, was shown to be a potent cysteine protease inhibitor.[3] Subsequent exhaustive studies on structure–activity relationships[4–9] led to the design of a clinically usable drug ethyl (+)-(2*S*,3*S*)-3-{1-[*N*-(3-methylbutyl)amino]leucylcarbonyl}oxirane-2-carboxylate (loxistatin) (**3**), which is a potent cysteine protease inhibitor derived from (**2**) (E-64-c).[10]

To facilitate the design of further highly potent drugs, it is essential to establish the three-dimensional structure of existing inhibitors, and in particular to identify those conformations which bind to the proteases.

Experimental

Materials.—Loxistatin was synthesized according to the method of Tamai and co-workers.[8] After various attempts to obtain single crystals, transparent needles suitable for *X*-ray analysis were crystallized from a dimethylformamide solution.

X-Ray Crystal Analysis.—A single crystal (dimensions being 0.1 × 0.1 × 0.5 mm^3) was used for the *X*-ray crystal analysis. Cell parameters were obtained from a least-squares fit of the

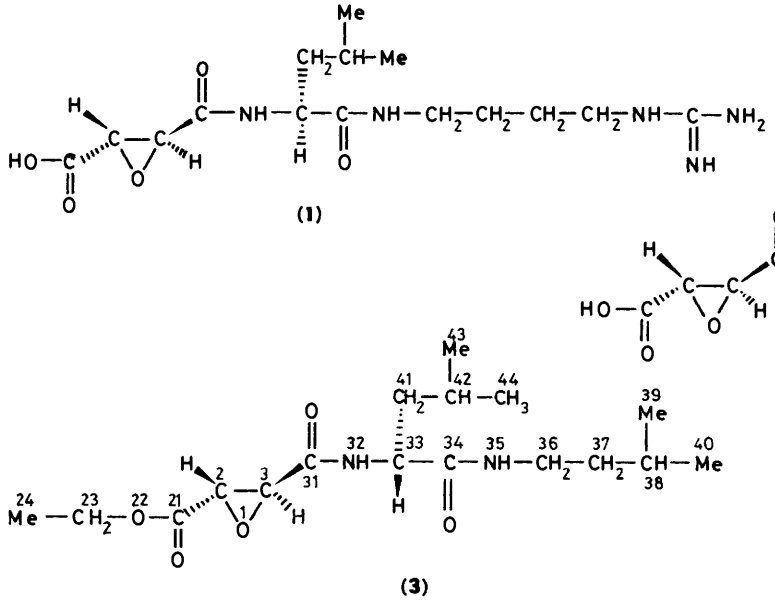

(1)

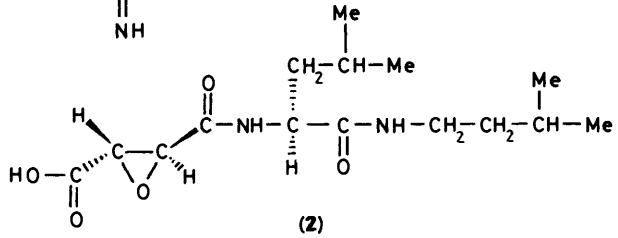

(2)

(3)

setting angles of 45 reflections measured on a Rigaku AFC-5 diffractometer with graphite-monochromated Cu-K_α radiation (λ = 1.5405 Å). Crystal data were obtained as follows: $C_{17}H_{30}N_2O_5$, M = 342.43. Orthorhombic, space group $P2_12_12_1$, a = 4.856(2), b = 13.971(4), c = 29.28(1) Å, V = 1 987(1) Å^3, D_m = 1.142(2) (flotation in C_6H_6–CCl_4), D_c = 1.145 g cm^{-3}, Z = 4, μ(Cu-K_α) = 6.54 cm^{-1}, F(000) = 744.

X-Ray diffraction intensities within 2θ = 130° were measured by the same diffractometer employing the $\omega/2\theta$ scan technique with a scan speed of 3° min^{-1}; the scan width was (1.1 + 0.15tanθ)° (at ω-circle) with 3 s backgrounds measured at the two extremes of the scan peak. The intensities of four standard reflections measured every 100 reflections remained constant to within 1% of their mean values. The measured intensities were then subjected to Lorentz and polarization corrections; no correction was applied for absorption effect because of the small crystal size used, and because of there being no significant intensity variation of a reflection for the φ scan at χ = 90°. Out of 2 019 independent intensities, 1 749 having $F_o^2 \geqq 3\sigma(F_o)^2$ were considered as observed and were used for the following structure determination and refinement, where $\sigma(F_o)^2$ is the standard deviation based on counting statistics.

The structure was solved by the direct method using the RANTAN program.[11] An *E*-map calculated using a phase set of 450 reflections ($E > 1.18$) with the highest combined figure of merit revealed the geometrically acceptable positions of the loxistatin non-hydrogen atoms. The structure was then refined by the full-matrix least-squares method with isotropic thermal parameters, and then by the block-diagonal least-squares method with anisotropic ones. The ideal positions of all hydrogen atoms were calculated, verified on a difference Fourier map, and then included in the refinement with an overall isotropic thermal parameter (4.4 Å^2). The function minimized was $\Sigma w(|F_o| - |F_c|)^2$, where $|F_o|$ and $|F_c|$ are the observed and calculated structure amplitudes, respectively. The weighting scheme used for the last refinement was as follows: $w = 1.0/[\sigma(F_o)^2 - 0.128\,95|F_o| + 0.010\,14|F_o|^2]$. Discrepancy indexes R ($= \Sigma||F_o| - |F_c||/\Sigma|F_o|$) and R_w ($= [\Sigma w(|F_o| - |F_c|)^2/\Sigma w|F_o|^2]^{1/2}$) were 0.064 and 0.079, respectively; and S (goodness of fit) $\{= [w(|F_o| - |F_c|)^2/(M - N)]^{1/2}$, (where M = number of observed reflections and N = number of variables)$\}$ was 1.98. None of the positional parameters shifted more than one fifth of their standard deviations, and maximum electron density in the final Fourier synthesis was 0.29 e Å^{-3}.

For all crystallographic computations, the UNICS programs[12] were used, and atomic scattering factors and terms of the anomalous dispersion correction were from International Tables for *X*-ray Crystallography.[13] The computational calculations were performed on an ACOS-1000 computer at the Computation Center of Osaka University. Final atomic co-ordinates for the non-hydrogen atoms are given in Table 1.*

^{1}H *N.m.r. Measurements.*—^{1}H N.m.r. spectra were measured on a Varian XL-300 (300 MHz) spectrometer equipped with fast FT and temperature-controlled (the error is within ±0.1 °C) units.

Loxistatin dried for one day under a reduced desiccator was dissolved in $CDCl_3$ and $(CD_3)_2SO$ solutions. The concentrations were then gravimetrically adjusted to *ca.* 0.05M. Proton chemical shift (δ) was measured as a downfield shift from the internal tetramethylsilane (TMS); the estimated standard error was ±0.001 p.p.m. (±0.3 Hz). All the proton resonances of loxistatin were assigned by spin multiplicities, homonuclear decouplings, and two-dimensional proton–proton correlations.

The conformation of the loxistatin molecule was estimated by using the coupling constants between protons (J) and the following three equations:

$J_{NHC_\alpha H} = 7.9\ \cos^2\theta - 1.5\ \cos\theta + 1.3\ \sin^2\theta$ (1)[14] for the torsion angle θ of H–N(32)–C(33)–H

$\Sigma J_{HNC_\beta H_2} = 6.0\ \cos^2\varphi - 1.5\ \cos\varphi + 12.5\ \sin^2\varphi$ (2)[15] for the torsion angle φ of C(34)–N(35)–C(36)–C(37)

and $J_{HC_\alpha C_\beta H} = 11.0\cos^2\theta - 1.4\cos\theta + 1.6\sin^2\theta$ (3)[16] for the torsion angle θ of H–C(33)–C(41)–H

The possible torsion angles of H–C(36)–C(37)–H, H–C(37)–C(38)–H, and H–C(41)–C(42)–H were estimated from a vicinal coupling constant–dihedral angle map modified by Bothner-By[17] and Garbisch[18] based on the Karplus equation of $J = A + B\cos\theta + C\cos2\theta$.[19] In contrast, the possible conformation around the C(3)–C(31) or C(33)–C(34) bonds was estimated by the nuclear Overhauser effect (n.O.e.) measurements of the 2-H and 3-H with respect to the 32-H, or the 33-H, 42-H, and 36-H with respect to the 35-H, respectively. Solutions for n.O.e. measurements (0.05M) were degassed with four freeze–pump–thaw cycles directly in n.m.r. tubes, which were then sealed. N.O.e. was measured by difference spectroscopy by acquiring both on- and off-resonance spectra and the enhancements were calculated from the integrated intensities of the peaks.

Table 1. Atomic co-ordinates of non-hydrogen atoms with their estimated standard deviations in parentheses

Atom	*x*	*y*	*z*
O(1)	0.645 0(6)	0.098 8(2)	0.580 19(7)
C(2)	0.655 1(8)	0.198 6(3)	0.589 2(1)
C(21)	0.836 9(8)	0.255 4(4)	0.558 4(1)
O(21)	1.024 7(6)	0.222 5(3)	0.536 80(9)
O(22)	0.766 2(7)	0.346 1(2)	0.559 53(7)
O(23)	0.938(1)	0.409 6(4)	0.530 9(2)
C(24)	0.857(2)	0.505 0(5)	0.542 2(2)
C(3)	0.787 4(7)	0.129 6(3)	0.620 0(1)
C(31)	0.650 8(6)	0.106 6(3)	0.664 9(1)
O(31)	0.401 9(5)	0.099 3(2)	0.668 48(8)
N(32)	0.825 9(5)	0.095 8(2)	0.699 44(8)
C(33)	0.738 6(6)	0.075 1(3)	0.746 3(1)
C(34)	0.862 5(7)	0.153 9(3)	0.776 3(1)
O(34)	1.112 4(5)	0.160 7(2)	0.780 26(8)
N(35)	0.684 1(6)	0.213 8(2)	0.795 63(9)
C(36)	0.771 9(8)	0.291 3(3)	0.825 6(1)
C(37)	0.839(1)	0.255 6(3)	0.873 9(1)
C(38)	0.978(1)	0.331 8(3)	0.904 0(1)
C(39)	0.803(1)	0.418 3(4)	0.910 2(2)
C(40)	1.056(1)	0.288 6(4)	0.949 1(1)
C(41)	0.833 4(9)	−0.025 1(3)	0.760 5(1)
C(42)	0.756(2)	−0.059 2(4)	0.807 0(2)
C(43)	0.581(3)	0.005 0(6)	0.831 2(2)
C(44)	0.841(2)	−0.161 9(4)	0.812 9(2)

Results and Discussion

Crystal Structure

Molecular Structure and Conformation.—A stereoscopic (ORTEP[20]) drawing of loxistatin is shown in Figure 1. The bond lengths and the angles between non-hydrogen atoms, and selected torsion angles, are listed in Tables 2 and 3, respectively.

Although some bond lengths and angles for the ester and for the leucyl and 3-methylbutyl atoms show unusual values

* *Supplementary data* (see section 5.6.3 of Instructions for Authors, in the January issue). Hydrogen-atom co-ordinates and thermal parameters have been deposited at the Cambridge Crystallographic Data Centre.

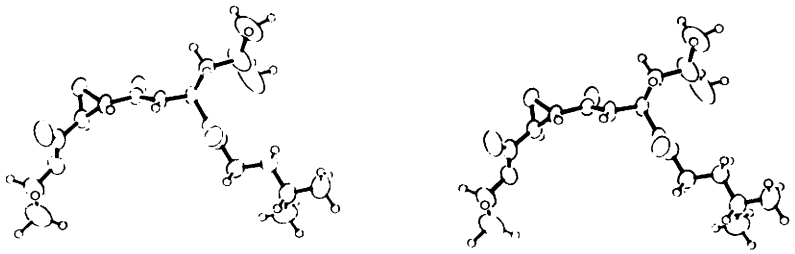

Figure 1. Stereoscopic drawing of loxistatin molecule observed in the crystal structure

Table 2. Bond lengths (Å) and angles (°) with their estimated standard deviations in parentheses

Bond lengths			
O(1)–C(2)	1.420(5)	O(1)–C(3)	1.422(5)
C(2)–C(3)	1.469(5)	C(2)–C(21)	1.490(6)
C(21)–O(21)	1.202(6)	C(21)–O(22)	1.314(6)
O(22)–C(23)	1.477(8)	C(23)–C(24)	1.41(1)
C(3)–C(31)	1.507(5)	C(31)–O(31)	1.218(5)
C(31)–N(32)	1.330(5)	N(32)–C(33)	1.464(5)
C(33)–C(34)	1.532(6)	C(33)–C(41)	1.531(6)
C(34)–O(34)	1.223(5)	C(34)–N(35)	1.331(5)
N(35)–C(36)	1.457(5)	C(36)–C(37)	1.535(6)
C(37)–C(38)	1.539(7)	C(38)–C(39)	1.490(8)
C(38)–C(40)	1.499(9)	C(41)–C(42)	1.483(9)
C(42)–C(43)	1.45(2)	C(42)–C(44)	1.49(1)
Bond angles			
C(2)–O(1)–C(3)	62.2(2)	O(1)–C(2)–C(3)	59.0(2)
O(1)–C(2)–C(21)	115.6(3)	C(21)–C(2)–C(3)	117.5(4)
C(2)–C(21)–O(21)	124.4(5)	C(2)–C(21)–O(22)	110.1(4)
O(21)–C(21)–O(22)	125.4(5)	C(21)–O(22)–C(23)	114.7(4)
O(22)–C(23)–C(24)	108.2(7)	O(1)–C(3)–C(2)	58.8(2)
O(1)–C(3)–C(31)	115.9(3)	C(2)–C(3)–C(31)	119.0(3)
C(3)–C(31)–O(31)	122.0(3)	C(3)–C(31)–N(32)	114.0(3)
O(31)–C(31)–N(32)	124.0(4)	C(31)–N(32)–C(33)	123.3(3)
N(32)–C(33)–C(34)	106.4(3)	N(32)–C(33)–C(41)	110.3(3)
C(34)–C(33)–C(41)	111.2(3)	C(33)–C(34)–O(34)	120.0(4)
C(33)–C(34)–N(35)	116.1(3)	O(34)–C(34)–N(35)	123.8(4)
C(34)–N(35)–C(36)	122.2(3)	N(35)–C(36)–C(37)	112.1(3)
C(36)–C(37)–C(38)	113.4(4)	C(37)–C(38)–C(39)	112.3(4)
C(37)–C(38)–C(40)	109.7(4)	C(39)–C(38)–C(40)	113.3(5)
C(33)–C(41)–C(42)	118.4(4)	C(41)–C(42)–C(43)	112.8(8)
C(41)–C(42)–C(44)	111.1(6)	C(43)–C(42)–C(44)	133.8(9)

Table 3. Selected torsion angles (°) with their estimated standard deviations

O(1)–C(2)–C(3)–C(31)	−104.4(4)
O(1)–C(2)–C(21)–O(21)	−21.9(7)
C(3)–C(2)–C(21)–O(21)	44.8(7)
C(2)–C(21)–O(22)–C(23)	178.7(4)
C(21)–O(22)–C(23)–C(24)	−168.8(6)
O(1)–C(3)–C(31)–N(32)	151.5(3)
C(2)–C(3)–C(31)–N(32)	−141.4(4)
O(31)–C(31)–N(32)–C(33)	−0.9(6)
C(31)–N(32)–C(33)–C(41)	113.4(4)
N(32)–C(33)–C(34)–N(35):ψ_1	113.1(4)
C(41)–C(33)–C(34)–N(35)	−125.9(4)
C(34)–C(33)–C(41)–C(42)	61.2(6)
O(34)–C(34)–N(35)–C(36)	−3.2(6)
N(35)–C(36)–C(37)–C(38)	170.2(4)
C(36)–C(37)–C(38)–C(40)	−175.4(4)
C(33)–C(41)–C(42)–C(44)	172.9(5)
C(21)–C(2)–C(3)–C(31)	150.9(4)
O(1)–C(2)–C(21)–O(22)	159.8(4)
C(3)–C(2)–C(21)–O(22)	−133.5(4)
O(21)–C(21)–O(22)–C(23)	0.4(7)
O(1)–C(3)–C(31)–O(31)	−28.9(5)
C(2)–C(3)–C(31)–O(31)	38.2(5)
C(3)–C(31)–N(32)–C(33):ω_1	178.7(3)
C(31)–N(32)–C(33)–C(34):φ_1	−124.2(4)
N(32)–C(33)–C(34)–O(34)	−64.7(5)
C(41)–C(33)–C(34)–O(34)	56.2(5)
N(32)–C(33)–C(41)–C(42):χ^{11}	179.9(5)
C(33)–C(34)–N(35)–C(36):ω_2	179.1(3)
C(34)–N(35)–C(36)–C(37):φ_2	−79.0(5)
C(36)–C(37)–C(38)–C(39)	60.2(6)
C(33)–C(41)–C(42)–C(44):χ^{21}	172.9(5)

because of their high thermal motions, those for the remaining atoms are in the acceptable range within their standard errors.[21] The epoxy ring has dimensions comparable with related compounds,[22] and allows dihedral angles of 96.9(6)° and 84.7(5)° with the neighbouring ester [C(21)–O(21)–O(22)] and peptide [C(31)–O(31)–N(32)–H(32)] planes. Both planes occupy a *trans* position with respect to the epoxy ring and the torsion angle of C(21)–C(2)–C(3)–C(31) is 150.9(4)° (Table 3); a common conformation can be seen in the orientation of the oxo groups with respect to the epoxy ring; the torsion angles of O(1)–C(2)–C(21)–O(21), C(3)–C(2)–C(21)–O(21), O(1)–C(3)–C(31)–O(31), and C(2)–C(3)–C(31)–O(31) bond sequences are −21.9, 44.8, −28.9, and 38.2°, respectively, *i.e.*, each C=O bond has a (*gauche*, *gauche*) orientation to the ring. Since energy calculations, using the CNDO/2 method,[23] showed this *gauche*-, *gauche* orientation to be in one of the energetically stable global regions, the conformation observed would be a characteristic of *trans* epoxysuccinyl compounds. The peptide groups are all *trans* and are nearly planar with $\Delta\omega$ values of 1.3° and 0.9° for the peptide bonds to left and right sides of the L-leucine residue. The backbone chain around the leucine residue takes a commonly observed conformation in many peptides,[24] and the (ψ_1, φ_1) angle is in a stable region of a Ramachandran plot.[25] The torsion angle φ_2 is in the frequently observed region for peptides containing a glycine residue.[24] The leucyl side-chain is also in a stable conformation, since the χ^{11} and χ^{21} values belong to a *trans* region, as in the majority of L-leucine structures that have been observed.[26] The 3-methylbutyl entity of the loxistatin terminal has a similar *trans* conformation to the leucyl side-chain. The *trans* conformation is also observed in the ester group at the other end of the molecule.

Judging from these torsion angles, the conformation of loxistatin seen in the crystal structure appears to be energetically stable, not affected by external factors such as crystal packing forces. Overall, the loxistatin conformation is best represented as a flattened, curved structure (see Figures 1 and

3), although there is no intramolecular hydrogen bond. The radius of the curvature is *ca.* 5.5 Å, and the thickness is *ca.* 3.5 Å; the leucyl side-chain lies almost on the *trans* zigzag plane of the loxistatin main chain.

Crystal Packing and Hydrogen Bonds.—Crystal packing viewed from the *a*-axis is shown in Figure 2, where hydrogen atoms are omitted for clarity. Four loxistatin molecules in a unit cell, which are related by diad screw symmetry, are linked to one another with no specific interaction force. Some weak van der Waals forces among the neighbouring ester entities and between the epoxy O(1) and 3-methylbutyl C(30) atoms stabilize the molecular packing in the *b*- and *c*-directions. A characteristic of loxistatin crystal packing is the formation of infinite parallel β-sheet structures along the *a*-direction. The molecular arrangement is shown in Figure 3. The respective N atoms of two peptide groups are hydrogen-bonded to the O atoms of the same groups translated by a unit cell to the *a*-axis: N(32) (at *x*, *y*, *z*) - - - O(31) (at *x* + 1, *y*, *z*) 2.940(5) Å, H(32) - - - O(31) 0.99(4) Å, and ∠N(32)–H(32) - - - O(31) 169(4)°; N(35) (at *x*, *y*, *z*) - - - O(34) (at *x* − 1, *y*, *z*) 2.909(4) Å, H(35) - - - O(34) 0.82(5) Å, and ∠N(35)–H(35) - - - O(34) 174(4)°. The pleat periodicity of this β-structure [C(3)–C(36) length] corresponds to 6.43 Å, and the distance between the pleated structures is 4.86 Å, which also equals the length of the *a*-axis. These data, together with the dihedral angle between the two peptide groups [113.9(6)°], are in the range normally observed in oligopeptides showing a parallel β-pleated sheet structure.[27] Since the longest axis of the loxistatin needle crystal coincides with the *a*-axis of the crystal structure, it would be reasonable to consider that the formation of infinite and regular β-sheet structures *via* NH–O hydrogen bonds is the main driving factor for the phase transition from the solution to the crystalline state.

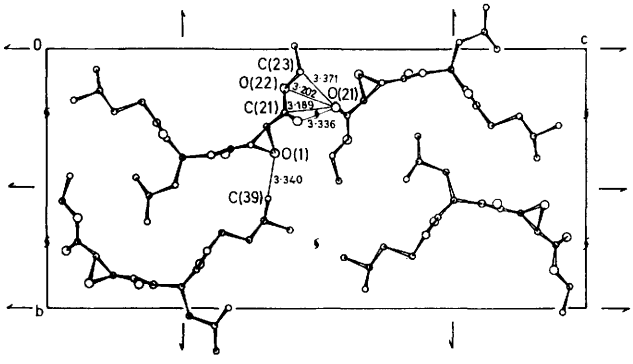

Figure 2. Crystal packing of loxistatin molecules viewed along the *a*-axis. Thin lines represent short contacts between neighbouring atoms

Solution Conformation

Using *X*-ray crystallographic analysis, the conformation of the loxistatin molecule was shown to be a flattened, curved structure. This conformation appears to represent a stable form, since the torsion angles around the bonds occupy energetically stable regions.

In order to confirm these results and to define further the

Table 4. Proton chemical shifts (at 31 °C) and temperature coefficients ($d\delta/dT \times 10^4$ p.p.m.·deg^{-1}) in $(CD_3)SO$ and $CDCl_3$ solutions

	$(CD_3)_2SO$		$CDCl_3$	
Proton	δ(p.p.m.)	$d\delta/dT$[a]	δ(p.p.m.)	$d\delta/dT$[a]
32-H	8.547	−67	6.617	−38
35-H	7.995	−57	6.003	−45
33-H	4.253	11	4.383	−10
23-H	4.187	1	4.266	−1
2-H[b]	3.716	2	3.678	−8
3-H[b]	3.575	3	3.460	−8
36-H	3.051	4	3.260	0
38-H, 42-H[c]	1.538	4	1.614	4
41-H	1.452	6	1.550	5
37-H	1.279	5	1.394	2
24-H	1.230	1	1.361	−3
39-H, 44-H[c]	0.884	1	0.914	2
43-H, 44-H	0.856	1		
	0.845	2		

[a] A negative value denotes a resonance that is more shielded at a higher temperature. [b] Assignment for the 2-H and 3-H is tentative, and therefore interchangeable. [c] These protons could not be separately assigned.

Table 5. Vicinal coupling constants (at 25 °C) and possible torsion angles comparable with the *X*-ray data

	^{1}H-n.m.r.				
	$(CD_3)_2SO$		$CDCl_3$		*X*-ray
Proton–proton	*J*(Hz)	θ(°)	*J*(Hz)	θ(°)	θ(°)
32-H—33-H	8.64	162	8.29	157	174
35-H—36-H[a]	11.48	−73	10.30	−61	−79
33-H—41-H[b]	7.25	31	6.85	34	63
		135	5.30	133	177
36-H—37-H[b]	7.00	40[c]	7.25	50[c]	55
		130	5.35	120	170
37-H—38-H[b]	7.17	40[c]		40[c]	78
		130		130	−168
41-H—42-H[b]	7.25	−40[c]		45[c]	−67
		−130		−125	−174

[a] *J* Values are the $\Sigma(^3J_{NH-CH})$, and the θ represents the C(34)–N(35)–C(36)–C(37) torsion angle φ. [b] *J* Values are the averaged ones among the vicinal protons. [c] These values correspond to the torsion angles of one of two 36-H, 37-H, or 41-H.

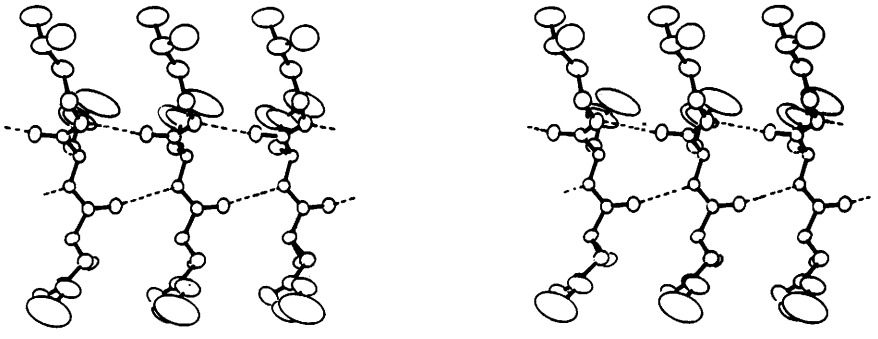

Figure 3. Stereoscopic drawing of the parallel β-sheet structure of the loxistatin molecules arranged along the *a*-axis

conformational characteristics of loxistatin, a ^1H n.m.r. analysis in $(CD_3)_2SO$ and $CDCl_3$ solutions was carried out.

Solvent and Temperature Dependences of NH Protons.—The participation of NH protons in intramolecular hydrogen bonding was examined by the temperature dependences of the NH chemical shifts in $(CD_3)_2SO$ and $CDCl_3$ solutions. The results are given in Table 4. As seen from Table 4, the behaviour of two NH protons is nearly identical: (i) the protons undergo upfield shifts of 1.9—2.0 p.p.m. upon a change in the solvent from $CDCl_3$ [the dipole moment μ 1.87 debye (D)] to $(CD_3)_2SO$ (μ 3.96 D) and, (ii) both NH protons show relatively large temperature coefficients ($d\delta/dT$) in both solvents. When these data are compared with those for other peptides,[28] it can be concluded that these NH protons do not participate in intramolecular hydrogen bonding. In contrast, the n.m.r. spectrum of loxistatin showed a noticeable concentration dependence; the mean chemical shift changes for the NH protons from 25mM—100mM in $(CD_3)_2SO$ solution at 31 °C were 0.06 and 0.08 p.p.m. for the 32-H and 35-H, respectively. The rates of deuterium exchange of the NH protons [upon the addition of D_2O (0.05 ml) to $(CD_3)_2SO$ (0.4 ml) solution] were both very slow at 25 °C, and the half-times ($t_{1/2}$) of deuteriation at 80 °C were 20.2 and 38.8 min for the 32-H and 35-H, respectively. These data, when compared with data for related systems,[28] suggest that the loxistatin molecules exist in solution as aggregates held together by intermolecular NH - - - O hydrogen bonds, such as are seen in Figure 3.

Possible Conformation.—There is no evidence for conformational heterogeneity on the n.m.r. time-scale. A possible conformation around respective N–C and C–C bonds can be estimated from the corresponding coupling constants and the equations shown in the Experimental section. The *J* values and the torsion angles comparable with the *X*-ray data are given in Table 5. The $^3J_{HNC,H}$ for 32-H—33-H and 35-H—36-H correspond near to 160° and −67° as the H–N(32)–C(33)–H and C(34)–N(35)–C(36)–C(37) torsion angles, respectively, and are in good agreement with the ones observed in the crystal structure (174 and −79°). Therefore it would be reasonable to suppose that the conformations around these bonds are similar to each other in the solution and crystalline states. In contrast the possible H–C–C–H torsion angles around C(36)–C(37), C(37)–C(38), C(33)–C(41), and C(41)–C(42) bonds are different between the solution and crystal states. The reason for this disagreement would be due in part to the relevance of the equations used for the estimation of torsion angles, and in part to the greater conformational freedom of these bonds in the solution state than in the solid state.

In order to deduce the whole conformation of the loxistatin molecule in solution, the conformation around C(3)–C(31) and C(33)–C(34) bonds had to be elucidated. To address this question, n.O.e. measurements were carried out in $CDCl_3$ solution. The irradiation of the 32-H showed positive n.O.e.s for the 2-H (9.0%) and 3-H (8.7%). The occurrence of almost similar n.O.e. effects implies that the distance of 32-H—2-H is almost equal to that of 32-H—3-H; the torsion angle of C(2)–C(3)–C(31)–N(32) is estimated to be *ca.* −60°. In contrast, the irradiation of the 35-H showed 8.6 and 3.6% positive n.O.e.s for the 33-H and 36-H, respectively. The strong n.O.e. of the 33-H, compared with that of 36-H, suggests that the C(33)–H(33) and N(35)–H(35) bonds are parallel to each other, and that therefore, the N(32)–C(33)–C(34)–N(35) torsion angle is close to 120°; this value is very near to that (113.1°) in a crystal structure. Similar n.O.e. results were also obtained in $(CD_3)_2SO$ solution, although their effects were not as significant as in $CDCl_3$ solution. Figure 4 shows a proposed solution conformation of the loxistatin molecule, based on the above n.m.r. data and assuming a *trans* peptide linkage. The configuration of the ester group to the epoxy ring is based on there being no n.O.e. effect between 23-H and 2-H or 3-H.

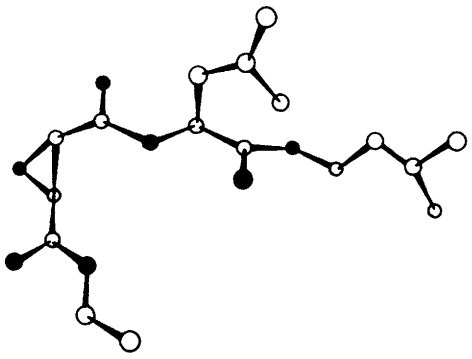

Figure 4. Schematic drawing of the proposed conformation of loxistatin in solution

Comparison of the Loxistatin Conformation in the Crystalline and Solution States.—Judging from the possible torsion angles around the respective bonds estimated by ^1H n.m.r. analyses, the backbone chain consisting of the C(3)–C(31)–N(32)–C(33)–C(34)–N(35)–C(36)–C(37) bond sequence appears to take an essentially similar conformation to the one observed in the crystal structure; respective torsion angles belong to one of the energetically stable regions in a Ramachandran plot.

The difference between the crystal and solution conformations is in the side and terminal chains of loxistatin; the torsion angles around the C(36)–C(37), C(37)–C(38), and C(41)–C(42) bonds in Table 5 are all near to the +synclinal or +anticlinal region in the solution, while the conformation corresponding to the latter region is varied to the *trans* form in the crystal structure. The two hydrophobic 2-methylpropyl groups, under conditions where the loxistatin molecules are surrounded with polar solvent, may prefer to take a folded form rather than the extended one observed in the crystal structure. Another difference is observed in the orientation of the peptide group consisting of C(32), O(31), N(32), and H(32) atoms with respect to the epoxy ring. The preference of the *gauche*, *gauche* orientation of the carbonyl group to the ring, suggested by *X*-ray analysis and energy calculations, was not observed in solution; the access of solvent molecules to O(1) and O(31) atoms would not allow the close contact of both the atoms by the electronic repulsions with the aprotic solvent Cl or O atom.

It may therefore be concluded that the loxistatin molecule has a relatively large degree of conformational freedom in solution, although the conformation of main backbone chain is relatively restricted compared to the side-chain.

Biological Implications of the Loxistatin Conformation.—It is of interest to consider why loxistatin acts as an inhibitor only for cysteine proteases such as papain and cathepsins. It has already been established[3,4] that the epoxy ring interacts with the cysteine residue which occurs in the active site of such proteases, and forms a stable thioether bond. Since the ester entity of loxistatin, which plays a role in elevating the absorption from digestive organs, is smoothly de-esterified to the highly active compound (**2**) (E-64-c) in the blood, the conformation of the L-leucyl and 2-methylpropylamino entities must determine whether or not the loxistatin molecule exhibits high inhibitory activity. These entities, in the form of the E-64-c–protease complex which involves a thioether linkage, show strong affinity for the 3-D structure of the protease active site.

Among cysteine proteases, papain,[29] actinidin,[30] and calo-

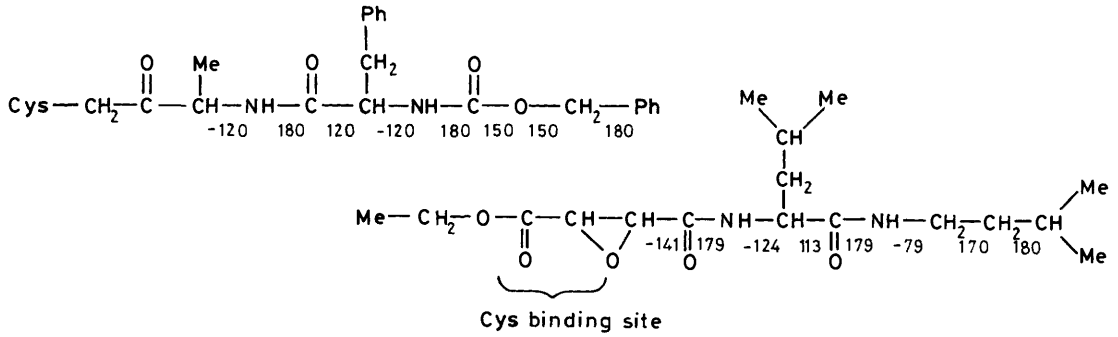

Figure 5. Conformational comparison between Bzl-Phe-Ala-methylene and loxistatin molecules observed in the crystal structure

tropic DI[31] have been subjected to *X*-ray crystallographic analyses, and these enzymes show structural similarity. Furthermore, the structures of the papain–substrate analogue complexes have also been reported; the benzyloxycarbonyl-(Bzl)-Phe-Ala-, Bzl-Gly-Phe-Gly-, and Acetyl-Ala-Ala-Phe-Ala-chloromethyl ketones substrate analogues all show similar conformations to one another at the papain active site.[32] Therefore, it is interesting to compare the conformations of these analogues with that of loxistatin. The torsion angles of Bzl-Phe-Ala-methylene covalently connected with the S^{γ} atom of Cys-25, which were directly estimated from Figure 3 in reference 32, are given in Figure 5, together with those of loxistatin observed in the crystal structure. From comparison of the substrate analogue (Bzl-Phe-Ala-CH_2-) with the inhibitor (loxistatin), the following two differences are seen: (i) the group binding to the cysteine residue exists on the *N*-terminal side for loxistatin, whilst it exists on the *C*-terminal side for Bzl-Phe-Ala-CH_2-; (ii) a significant difference in the torsion angles of both molecules is seen between the –CO–CH– (Bzl-Phe-Ala-CH_2-) and the corresponding –NH–CH– (loxistatin) bonds, and between –CH–NH– and –CH–CO– bonds: respective torsion angles are approximately related by mirror symmetry. These structural and conformational differences may form the basis for the discrimination between substrate and inhibitor molecules. The groove of the papain active site runs across the surface of the molecule,[29,32] and appears to have sufficient space to accommodate the conformation of loxistatin as observed by *X*-ray crystallographic or ^{1}H n.m.r. analysis.

The conformational comparison of Bzl-Phe-Ala-CH_2- with loxistatin has led us to consider an interesting idea; although the particular torsion angles are different from each other, the overall conformations of both molecules are similar as both exist as curved sheets, in which the C=O and N–H bonds project perpendicular to the sheet. The side-chain of the phenylalanine (for Bzl-Phe-Ala-CH_2-) or the leucine (for loxistatin) residue is extended from the main chain without significant deviation from the sheet. Since it has been generally accepted that the enzymatic reaction of cysteine proteases proceed *via* the formation of a Michaelis complex with the substrate, the formation of a covalent acyl-enzyme linkage followed by deacylation,[32] this conformational characteristic appears to be important for the formation of a stable Michaelis complex with cysteine proteases. In the case of loxistatin, the subsequent formation of the thioether linkage (instead of reversible acylation) between the epoxy ring and the active site cysteine residue leads to irreversible inactivation. We are now investigating the conformational characteristics of the related cysteine inhibitors such as (**1**) (E-64) and leupeptin in order to confirm that they are similar to loxistatin.

References

1 E. Reich, D. B. Rifkin, and E. Shaw, 'Proteases and Biological Control,' Cold Spring Harbor Laboratory, Cold Spring, New York, 1975; R. D. Berlin, H. Herrmann, I. H. Lepow, and J. M. Tanzer, 'Molecular Basis of Biological Degenerative Processes,' Academic Press, New York, 1978; A. J. Barrett, 'Proteinases in Mammalian Cells and Tissues,' Elsevier, North-Holland Biomedical Press, Amsterdam, 1977.
2 H. Sugita, *Medicina (Tokyo)*, 1985, **22**, 282.
3 K. Hanada, M. Tamai, M. Yamagishi, S. Ohmura, J. Sawada, and I. Tanaka, *Agric. Biol. Chem.*, 1978, **42**, 523; K. Hanada, M. Tamai, S. Ohmura, J. Sawada, T. Seki, and I. Tanaka, *ibid.*, p. 529.
4 K. Hanada, M. Tamai, S. Morimoto, T. Adachi, K. Oguma, S. Ohmura, and M. Ohzeki, 'Peptide Chemistry,' ed. H. Yonehara, Protein Research Found., 1980, p. 31.
5 K. Hanada, T. Tamai, S. Morimoto, T. Adachi, S. Ohmura, J. Sawada, and I. Tanaka, *Agric. Biol. Chem.*, 1978, **42**, 537.
6 A. J. Barrett, A. A. Kembhavi, M. A. Brown, H. Kirschke, C. G. Knight, M. Tamai, and K. Hanada, *Biochem. J.*, 1982, **201**, 189.
7 M. Tamai, T. Adachi, K. Oguma, S. Morimoto, K. Hanada, S. Ohmura, and M. Ohzeki, *Agric. Biol. Chem.* 1981, **45**, 675.
8 M. Tamai, K. Hanada, T. Adachi, K. Oguma, K. Kashiwagi, S. Ohmura, and M. Ohzeki, *J. Biochem.*, 1981, **90**, 255.
9 K. Suzuki, *J. Biochem.*, 1983, **93**, 1305.
10 K. Hanada, M. Tamai, T. Adachi, K. Oguma, K. Kashiwagi, S. Ohmura, E. Kominami, T. Towatari, and N. Katsunuma, 'Proteinase Inhibitors: Medical and Biological Aspects,' ed. N. Katsunuma, Japan Scientific Society Press, Tokyo/Springer-Verlag, Berlin, 1983, p. 25.
11 J. Jia-Xing, *Acta Crystallogr., Sect. A*, 1981, **37**, 642; 1983, **39**, 35.
12 The Universal Crystallographic Computing System-Osaka, The Computer Center, Osaka University, Osaka, Japan, 1979.
13 'International Tables for *X*-ray Crystallography,' eds. J. A. Ibers and W. C. Hamilton, Kynoch Press, Birmingham, 1974, vol. 4, pp. 99, 149.
14 G. N. Ramachandran, R. Chandrasekaran, and K. D. Kopple, *Biopolymers*, 1971, **10**, 2113.
15 K. D. Kopple, A. Go, R. H. Logan, and J. Savrda, *J. Am. Chem. Soc.*, 1972, **94**, 973.
16 K. D. Kopple, G. R. Wiley, and R. Tauke, *Biopolymers*, 1973, **12**, 627.
17 A. B. Bothner-By, *Adv. Magn. Reson.*, 1965, **1**, 195.
18 E. W. Garisch, Jr., *J. Am. Chem. Soc.*, 1964, **86**, 5561.
19 M. Karplus, *J. Am. Chem. Soc.*, 1963, **85**, 2870.
20 C. K. Johnson, ORTEP-II: A Fortran Thermal-Ellipsoid Plot Program for Crystal Structure Illustrations, ORNL-5138, Oak Ridge National Laboratory, 1976.
21 O. Kennard, 'International Tables for *X*-ray Crystallography,' eds. C. H. MacGillavry and G. D. Rieck, Kynock Press, Birmingham, 1968, vol. 3, p. 276.
22 For examples, see P. Murray-Rust, R. C. Glen, and R. F. Newton, *Acta Crystallogr., Sect. B*, 1982, **38**, 2698; N. Ebby, J. Lapasset, L. Pizzala, and H. Bodot, *ibid.*, p. 3128; K. P. Burns, G. Englert, R. Kazlauskas, P. T. Murphy, P. Schonholzer, and R. J. Wells, *Aust. J. Chem.*, 1983, **36**, 171; P. Murray-Rust, R. C. Glen, and R. F. Newton, *Acta Crystallogr., Sect.* B, 1982, **38**, 2702.
23 J. A. Pople and G. A. Segal, *J. Chem. Phys.*, 1966, **44**, 3289.
24 I. L. Karle, 'The Peptides, Analysis, Synthesis, Biology,' eds. E. Gross and J. Meienhoffer, Academic Press, New York, 1981, vol. 4, p. 1.
25 G. N. Ramachandran, C. Ramakrishnan, and V. Sasisekharan, *J. Mol. Biol.*, 1963, **7**, 95.
26 V. Cody, 'Chemistry and Biochemistry of the Amino Acids,' ed. G. C. Barrett, Chapman and Hall, London, 1985, p. 625.

27 T. Ashida, T. Yamane, and I. Tanaka, *J. Crystallogr. Soc. Jpn.*, 1980, **22**, 187.
28 A. B. Mauger, O. A. Stuart, R. J. Highet, and J. V. Silverton, *J. Am. Chem. Soc.*, 1982, **104**, 174; B. J. Rawson, J. Feeney, B. J. Kimber, and H. M. Greven, *J. Chem. Soc., Perkin Trans. 2*, 1982, 1471; K. D. Kopple, K. K. Bhandary, G. Kartha, Y.-S. Wang, and K. N. Parameswaran, *J. Am. Chem. Soc.*, 1986, **108**, 4637; G. R. Beilharz, J. Fong, P. O. L. Mack, A. V. Robertson, and P. E. Wright, *Aust. J. Chem.*, 1983, **36**, 751; T. Higashijima, J. Kobayashi, U. Nagai, and T. Miyazawa, *Eur. J. Biochem.*, 1979, **97**, 43; L. Zetta and F. Cabassi, *ibid.*, 1982, **122**, 215; B. P. Rogues, C. Garbay-Jaureguiberry, S. Bajusz, and B. Maigret, *ibid.*, 1980, **113**, 105.
29 I. G. Kamphnis, K. H. Kalk, M. B. A. Swarte, and J. Drenth, *J. Mol. Biol.*, 1984, **179**, 233.
30 E. N. Baker, *J. Mol. Biol.*, 1980, **141**, 441.
31 U. Heinemann, G. P. Pal, R. Hilgenfeld, and W. Saenger, *J. Mol. Biol.*, 1982, **161**, 591.
32 J. Drenth, K. H. Kalk, and H. M. Swen, *Biochemistry*, 1976, **15**, 3731.

Received 14*th April* 1987; *Paper* 7/674